EVALUATION AND PARAMETERS AFFECTING OF HYBRID ACTIVE CARBONE-ETHANOL SOLAR ADSORPTION REFRIGERATOR

Adnan G.T. Al-Hasnawi[1, 2]

[1]Institute of Fluid Dynamic and Thermodynamic
Otto-von Guericke University, University Square 2, D-39106, Magdeburg, Germany.
[2]Electromechanical Engineering, University of Technology- Baghdad
Tal Muhammad 10066, Baghdad, Iraq, Adnan_tuaamah@yahoo.com

Received 18 August 2025
Accepted 18 November 2025
DOI: 10.59957/jctm.v61.i3.2026.9

ABSTRACT

The development of environmentally acceptable refrigerants and the use of solar energy and low-grade waste heat made adsorption refrigerators more appealing. However, more study is required to optimize these methods further as they do not yet match the performance and commercial application of typical vapor compression systems. This article illustrates the thermal response of adsorption systems under varying operating circumstances by simulating the pressure effect on temperature distribution in a porous adsorbent bed using ANSYS Fluent. Although heat transfer in porous media has been studied in the past, little is known about the precise function that pressure plays in influencing thermal behaviour. According to simulation studies, ethanol desorption efficiency is increased by greater inlet pressures because they provide more consistent and raised temperature distributions. varied x-positions (2.9125 mm, 5.825 mm, and 11.65 mm) exhibit varied temperature profiles, which correspond to localized flow and pressure conditions. The results provide important insights into improving the design and functionality of adsorption-based cooling and separation systems by highlighting the predominant roles of heat conduction and vapor transport in determining thermal gradients.

Keywords: CFD, active carbon, ethanol, adsorption process.

INTRODUCTION

Adsorption refrigeration systems have garnered a lot of attention lately since they employ environmentally benign refrigerants and can run on solar energy or low-grade waste heat. In terms of effectiveness and commercial use, these systems are still unable to match traditional vapor compression refrigeration systems. Research in this field is therefore still ongoing with the goal of overcoming constraints related to technology, finances, and the environment.

The literature indicates that the choice of working pairs such as silica gel-water, activated carbon-methanol, activated carbon-ethanol, and zeolite-water-the heat source's temperature, and the materials' adsorption capacity are important variables that affect how well adsorption cooling systems perform. The necessity for effective energy use has grown increasingly pressing as the world's energy consumption keeps rising. In this regard, adsorption systems offer a viable substitute for sustainable energy management since they can function using low-grade thermal energy from sources like waste heat or solar energy [1]. A thermodynamic model of a two-bed Solar Adsorption Cooling system using an isothermal adsorption process was developed to improve efficiency. The 500 W chiller, with ethanol/activated carbon as the working pair, achieved a maximum COP of 0.68 at 95°C desorption temperature. This approach enhanced performance by 13.23 % compared to traditional isobaric methods [2]. A thermodynamic model showed that increasing adsorption time in a solar adsorption refrigeration system improves cooling capacity but lengthens cycle time, affecting overall efficiency. The optimal adsorption time was 71 minutes, with a COP of 0.476 and SCP of 28.6 W kg^{-1} [3]. A SIMULINK model of a two-bed adsorption cooling

system showed a COP of 0.57 at 80°C hot water inlet, with cooling and hot water temperatures significantly affecting performance. The system cooled 13.5 kW using 45 kg adsorbent and a 20 s switching time [4]. An adsorption ice generator using a composite adsorbent achieved a COP of 0.3046 and 33.27 kg ice kg^{-1} ads day^{-1} at optimal layer thickness and cycle time. Increasing thickness improved thermal conductivity but hurt efficiency due to higher mass transfer resistance [5]. A solar-powered adsorption ice system with aluminium foam-packed beds and Maxsorb adsorbent achieved 26 % higher ice production and COP compared to traditional finned-tube designs. Optimal results were 49 kg ice kg^{-1} adsorb 49 kg ice kg ads^{-1}ent in 8 h and a COP of 0.366 at specific foam thicknesses and cycle times [6]. A CFD based approach was developed to accurately estimate adsorption rate parameters for granular activated carbon filters, reducing the need for extensive experiments. The model successfully predicted adsorption rates and performance across different filter shapes made from the same material [7]. An ideal cycle study evaluated eight activated carbon-refrigerant pairs for adsorption cooling, finding Maxsorb-III/methanol to perform best with a COP of 0.803 and high specific cooling energy at 80°C desorption. KOH6-PR/ethanol and WPT-AC/ethanol also showed strong performance, while SAC-2/R32 underperformed despite a large concentration difference [8]. A CFD study modelled CO_2 hydrogenation to methanol using membrane reactors with NaA zeolite membranes to selectively remove water, shifting equilibrium and boosting conversion. This approach improved methanol yield by 16 % and CO_2 conversion by 20.6 % compared to traditional reactors, offering key insights for large-scale CCU [9]. An innovative stacked adsorber design using activated carbon and copper foils was modeled to improve heat and mass transfer in thermally powered adsorption heat pumps. The system achieved a heating COP of 1.36 and specific heating power of 762.6 W kg^{-1}, outperforming traditional adsorption systems for sustainable home heating [10].

Equilibrium adsorption characteristics of a gas or a vapour upon a solid can be presented by adsorption isotherms ($X = f(P)_T$), adsorption isobars ($X = f(T)_p$), and adsorption isosters ($P = f(T)_x$). In this work, the experimental study [11] was reproduced and simulated using ANSYS Fluent, a computational fluid dynamics (CFD) tool is used. The primary objective of this simulation is to investigate the effect of pressure on the temperature distribution within porous media. While previous studies have explored heat transfer and fluid flow in porous structures, they have not sufficiently addressed how variations in pressure influence the thermal behavior inside such media. This study aims to fill that gap by providing a detailed analysis of temperature distribution under different pressure conditions. The simulation results are expected to offer new insights that complement and extend the findings of Jribi wt al., contributing to a more comprehensive understanding of heat transfer mechanisms in porose media [11].

Working principle of adsorption cooling system

The four primary parts of the adsorption cooling system are an evaporator, a condenser, an expansion valve, and an adsorber/desorber bed loaded with activated carbon (generator). Pre-heating, desorption, pre-cooling, and adsorption are the four main processes that make up the system's operation. The bed is separated from the evaporator during the pre-heating phase, and hot water is pumped around to raise the pressure inside the bed. The desorption process starts when the bed pressure rises over the condenser's pressure. The active carbon (AC) releases ethanol vapor, which travels to the condenser and liquefies there. The bed's temperature and pressure are lowered during the pre-cooling phase by circulating cooling water after desorption. The system moves into the adsorption phase when the pressure falls below that of the evaporator. The active carbon (AC) in the bed adsorbs the ethanol vapor from the evaporator, creating a cooling effect. The heat of adsorption can be eliminated with the use of a steady flow of cooling water. The schrotric diagram of the adsorption cooling system with the adsorbent bed (generator) is displayed in Fig. 1.

Computational modelling

The porous zone needs to be created in the geometry and mesh stages of ANSYS Fluent before it can simulate flow through a porous media. The mesh is created (ICEM CFD) and then export to Fluent, where the porous area is designated as a distinct cell zone. Navigating to the cell zone condition panel, choosing the porous region, and turning on the (Porous Zone) and (Source Terms) option in Fluent will activate the porous media model

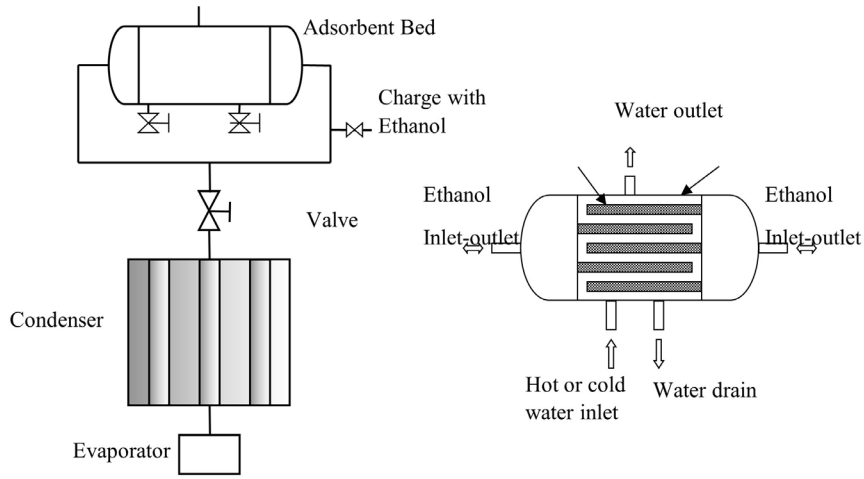

Fig. 1. Solid - vapour adsorption cooling system, Adsorbent Bed.

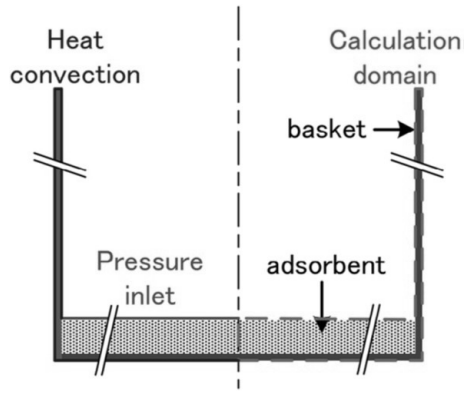

Fig. 2. Schematic of basket and adsorbent showing calculation domain and boundary conditions [11].

and adsorption desorption process. After that, the inertial resistance coefficient and viscous resistance (the inverse of permeability) with porosity and material type have to setup, which take into consideration pressure losses brought on by inertial and viscous effects, respectively. Other factors like thermal conductivity must also be mentioned.

The pressure-based solver is employed, and the flow regime determines which viscous model laminar is chosen. The energy and species models should activate. After starting the simulation, the solution is executed until convergence is achieved.

Simulation methodology

In the simulation, a cylindrical stainless-steel basket filled with activated carbon is suspended from a magnetic balance, as described in Fig. 2 [11]. Fig. 2 also provides a schematic representation of the adsorbent, basket configuration, and the boundary conditions applied in the simulation. The structure meshes give the user more control than the unstructured meshes, which is another grid technique advantage. In addition to supporting a high degree of skewness and stretching before effecting solution, hexahedral cells are highly effective at filling spaces. Furthermore, the grid is flow aligned, which facilitates post-processing and aids in solver convergence because logical grids serve as great points of reference for analysing the flow field. The drawback of structured mesh is that, in comparison to unstructured mesh, it takes too long to produce. Therefore, a structured hexahedral mesh is generated using the multi-block approach in ANSYS ICEM 2024

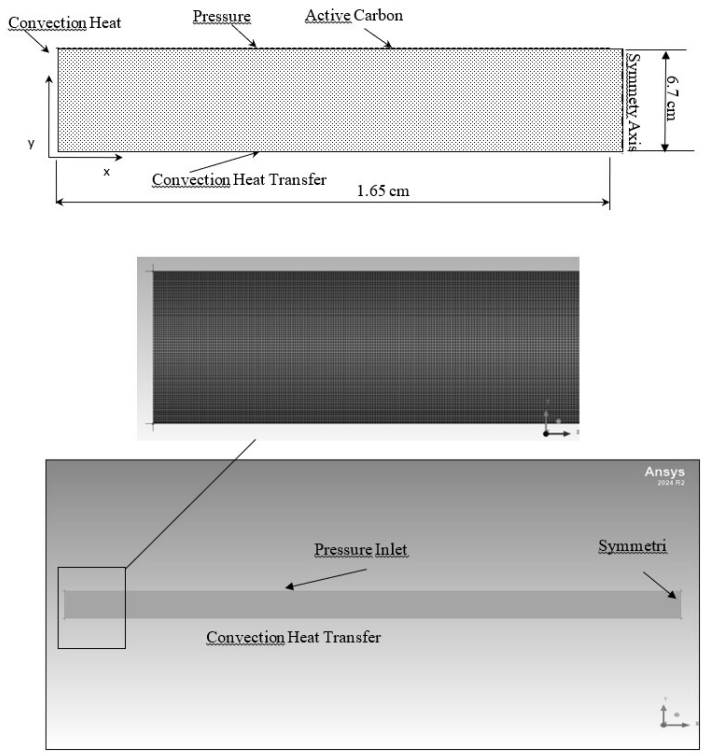

Fig. 3. Physical domain and coordinates.

R2. The mesh size consists of 80160 nodes and 7937 quads, providing adequate resolution for capturing the geometry and flow behaviour in the simulation domain. Mesh independence is proven to ensure numerical accuracy.

The coordinate system and physical domain of the computational domain utilized in this investigation are depicted in Fig. 3. To apply boundary conditions and explain flow behaviour, the coordinate system is defined to line up with the cylindrical basket's axis. Mass and heat transport between the vapor phase and the porous adsorbent bed can be accurately simulated thanks to the computational domain's inclusion of the surrounding fluid region. With this configuration, the simulation is guaranteed to accurately represent the physical processes taking place in the adsorption system. To exploit the system's geometric symmetry and lower computational costs, a symmetry boundary condition is added along the domain's central axis. The sec and third bounds, which are both modelled as walls with constant temperature, represent the outside surfaces of the adsorbent basket and the surrounding walls in the computational domain. Vapor can enter the domain under regulated pressure circumstances since the upper wall of the domain is designated as a pressure intake. These boundary conditions are chosen with care to provide realistic modelling of heat and mass transport processes inside the domain and to faithfully reproduce the physical behaviour of the adsorption system.

The thermodynamic and transport properties of ethanol are imported into ANSYS Fluent using Fluent database. The Active carbon heat capacity is 0.9 kJ kg^{-1} K^{-1}. The temperature and pressure of initial and boundary condition is ranging from 30°C to 70°C and 1.713 to 8.001 kPa respectively, ρ = 464.1 kg m^{-3} and porosity Φ = 0.4075 [11]. Regarding permeability and internal resistance, they can be calculated using Eq. (8) and Eq. (9), which are as follows:

$\alpha = 6.297 \times 10^{-12}$ m^2 and $C_2 = 4.378 \times 10^5$.

Because flow through porous media with small

particle sizes usually has a low Reynolds number, it is assumed that the flow inside the activated carbon bed is laminar. The vapor's low velocity and considerable flow resistance as it moves through the packed bed's tiny pores support this idea. To precisely depict the viscous-dominated behaviour inside the porous adsorbent region, the laminar flow model is turned on in ANSYS Fluent during the simulation. This guarantees accurate estimates of mass transfer, velocity distribution, and pressure drop during the adsorption process.

Equations in ANSYS fluent

The momentum and continuity equations must be solved in order to perform the CFD simulation. The equation of mass conservation, or continuity, can be expressed as shown in the ANSYS Fluent Theory Guide Eq. (1), where the rate of change of density and the net mass flux through a control volume must [12]:

$$\frac{\partial \rho}{\partial t} + \nabla (\rho \vec{v}) = S_m \quad (1)$$

The conservation of momentum in an internal reference frame shows how a fluid's momentum varies over time in response to forces such as pressure, viscous stresses, gravity, and external body forces. This relationship is mathematically stated as Eq. (2):

$$\frac{\partial}{\partial t} (\rho \vec{v}) + \nabla (\rho \vec{v} \vec{v}) = -\nabla p + \nabla (\tau) + \rho \vec{g} + \vec{F} \quad (2)$$

where ρ is the density, v is the velocity, S_m is the source term,p is the static pressure (Pa), τ is the stress, F is the external body force, g is the gravity, t is the time [13].

The stress tensor τ depicts the internal viscous forces within a fluid, which vary based on the rate of deformation of the fluid constituents. It is defined in terms of the velocity gradient and viscosity, as indicated in Eq. (3):

$$\tau = \mu \left[(\nabla \vec{v} + \nabla \vec{v}^T) - \frac{2}{3} \nabla \vec{v} I \right] \quad (3)$$

where μ is the molecular viscosity, *I* is the unit tensor and the sec term on the right-hand side of the Eq. (3) is the effect of volume dilation.

If the problem involves heat transmission, the energy equation must be addressed. The energy equation must be included because this study deals with heat transport. The following energy equation Eq. (4) governs heat transmission in a fluid domain:

$$\frac{\partial}{\partial t} (\rho E) + \nabla \left(\vec{v} (\rho E + \rho) \right) = \nabla \left(k_{eff} \nabla T - \sum h \vec{J} + (\tau_{eff} \vec{v}) \right) + S_h \quad (4)$$

where E is the energy term, v is the velocity, ρ is the density, K_{eff} is the effective turbulent kinetic energy, T is the local temperature in Kelvin, h is the enthalpy for ideal gas, J is the diffusion flux, τ_{eff} is the effective stress tensor, S_h is the volumetric heat source term, t is the time [13].

The term E in the energy equation Eq. (4) denotes the total energy per unit mass. It comprises the enthalpy h, the pressure work term p, and the kinetic energy. This relationship is given by Eq. (5):

$$E = h - \frac{p}{\rho} + \frac{v^2}{2} \quad (5)$$

The enthalpy h is determined by adding a reference enthalpy hi and the integral of the specific heat capacity $c_{p.\,j}$ from a reference temperature T_{ref} to the present temperature T, as indicated in Eq. (6). T_{ref} is set at 298.15 K.

$$h = h_i \int_{T_{ref}}^{T} c_{p,j}\, dT \quad (6)$$

The following equation can be used to calculate the porosity φ of the medium, as shown in Eq. (7), where porosity is defined as the ratio of the total pore volume to the bulk volume, that is

$$\varphi = \frac{total\ pore\ volume}{bulk\ volume} \quad (7)$$

Eq. (8) and Eq. (9) can be used to determine the permeability α and internal resistance C_2 of the porous medium [11, 13]. These relationships are expressed as in Eq. (8) and (9):

$$\alpha = \frac{d_p^2 - \varphi^3}{150 * (1-\varphi)^2} \quad (8)$$

$$C_2 = \frac{3.5 - (1-\varphi)}{d_p * \varphi^3} \quad (9)$$

The equivalent particle diameter d_p, can be

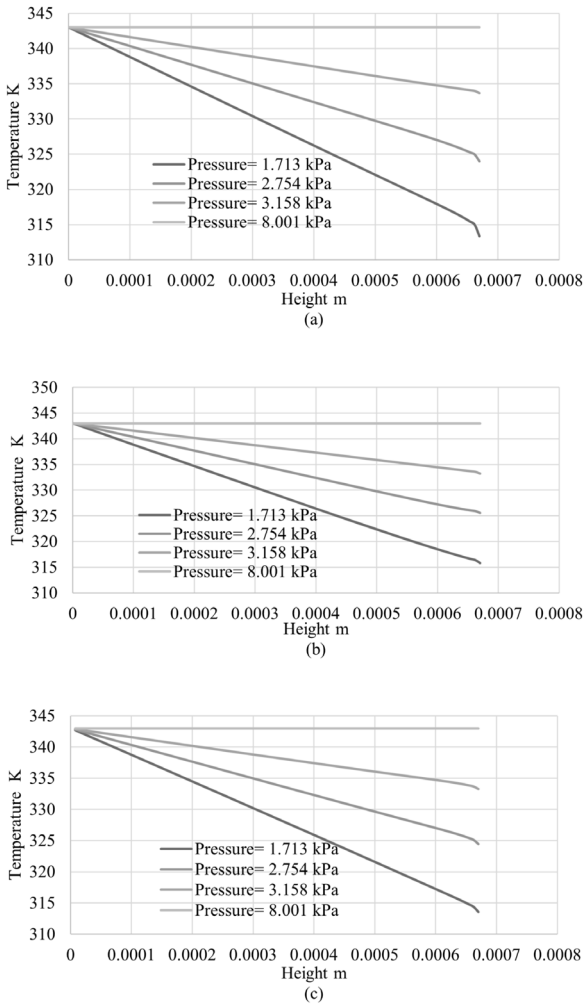

Fig. 4. Temperature distribution as a function to position (height m) and pressure (a) at x = 2.9125 mm (b) x = 5.825 mm and (c) x = 11.65 mm.

determined using Eq. (10) [12]. It is defined as the diameter of a sphere having the same volume as the particle:

$$d_p = \left(\frac{6}{\pi} V_{par.}\right)^{1/3} \quad (10)$$

RESULTS AND DISCUSSION

The effect of pressure on temperature distribution is shown in Fig. 4. The x-axis showing the position along the hight or thickness of the adsorbent bed in meter and the y-axis showing the temperature in K. The way heat moves through the porous structure during the desorption process is shown by this plot.

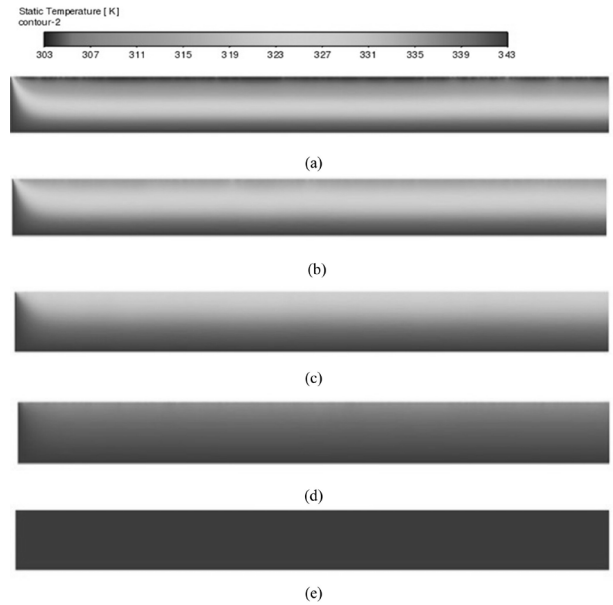

Fig. 5. Contour of temperature distribution as a function to pressure (a) at P = 1.713 kPa (b) P = 2.754 kPa, (c) P = 3.158 kPa, (d) P = 4.914 kPa, and (e) P = 8.001 kPa.

As heat is transferred from the heated wall into the porous material AC, a temperature gradient usually develops. Due to the endothermic nature of the process, the temperature may drop in the y-direction during desorption, but it rises as pressure increase.

In every situation where temperature changes in response to position (height) and pressure within the porous medium, this temperature distribution profile is seen. In particular, the profiles are assessed along the x-axis at three different points, at x = 2.9125 mm, x = 5.825 mm and x = 11.65 mm.

These sites correspond to various horizontal regions of the adsorbent bed. The temperature profile for each scenario illustrates how heat moves vertically through the porous media at a certain lateral point (in x-axes), impacted by the vapor flow conditions as well as conduction. Local temperature gradients are impacted by the desorption process, which is largely driven by the accompanying pressure distribution. By comparing these profiles, one can evaluate the impact of location and pressure on the system's heat and mass transfer efficiency as well as comprehend the spatial thermal behaviour within the bed.

Fig. 5 displays the temperature distribution contours as a function of pressure. It is evident that there is a direct relationship between the porous medium's thermal behaviour and inlet pressure. It is evident that the temperature rises in tandem with the pressure, especially in the adsorbent bed. A more even and elevated temperature distribution is the result of better heat transmission into the porous structure brought about by higher inlet pressure. Since higher temperatures make it easier for adsorbed ethanol molecules to be released from the activated carbon, this improved thermal uniformity is particularly advantageous for the ethanol desorption process. Consequently, raising the inlet pressure raises the system's total desorption efficiency in addition to improving the temperature field inside the bed.

CONCLUSIONS

- Inlet pressure and position have a significant impact on the temperature distribution inside the porous adsorbent bed.
- Temperatures rise and are distributed more evenly across the bed with higher pressure.
- The ethanol desorption process is more efficient because of this better heat distribution.
- Because of local pressure and flow circumstances, temperature profiles measured at various x-positions (2.9125 mm, 5.825 mm, and 11.65 mm) exhibit variance in heat transfer behaviour.
- Local temperature gradients within the porous media are determined in large part by heat conduction and vapor transport.
- A deeper comprehension of spatial thermal behaviour and the influence of pressure on heat and mass transfer performance is made possible by comparing temperature distributions across positions. These understandings are essential for improving the layout and functionality of cooling or separation systems based on adsorption.

Acknowledgments

I would like to express my heartfelt thanks to Otto von Guericke University, Magdeburg, Germany, and the University of Technology, Baghdad, Iraq, for their invaluable assistance and support throughout the course of this research work.

Authors' contributions

A.G.T. Al-Hasnawi: Conceptualization, methodology, data analysis, writing - original draft, data collection, writing.

REFERENCES

1. R.Z. Wang, R.G. Oliveira, Adsorption refrigeration an efficient way to make good use of waste heat and solar energy, International Sorption Heat Pump Conference, USA, 2005, 22-24.
2. A. Shaa, V. Baiju, Thermodynamic analysis and performance evaluation of activated carbon-ethanol two-bed solar adsorption cooling system, International Journal of Refrigeration, 123, 2021, 81-90.
3. Z. Wang, Z. Yuan, Z. Liu, Y. Liu, M. Bernat, Dynamic variation of bed parameters and time optimisation of solar adsorption refrigeration system based on CFD simulation, Applied Thermal Engineering, 235, 2023, 121405.
4. V. Baiju, A.A. Sha, N.M. Sajid, K. M. Shafeeque, Simulation and performance study of a two-bed adsorption cooling system operated with activated carbon-ethanol, J. of Mech. Eng. Science, 236, 7, 2022, 3804-3817.
5. M.B. Elsheniti, M.S. Eissa, H. Al-Ansary, J. Orfi, A. El-Leathy and O. Elsamni, Using a combination of activated carbon and graphene nanoparticles in a consolidated form for adsorption ice maker: a system-level modelling, MDPI, Appl. Sci., 12, 2022, 7602.
6. M.B. Elsheniti, M.S. Eissa, H. Al-Ansary, J. Orfi, O. Elsamni,A. El-Leathy, Examination of using aluminum-foam/finned-tube beds packed with maxsorb III for adsorption ice production system, MDPI Energies, 15, 2022, 2757.
7. Y. Kasai, Y. Jinbo, H. Kamikawa, T. Sanada, CFD modeling of adsorption rate prediction for granular activated carbon packed bed, J. of Chemical Engineering of Japan, 56, 2023, 2172980.
8. F. Shabir, M. Sultan, Y. Niaz, M. Usman, S.M. Ibrahim, Y. Feng, B.K. Naik, A. Nasir and I. Ali, Steady-state investigation of carbon-based adsorbent-adsorbate pairs for heat transformation application, MDPI, Sustainability, 12, 2020, 7040.

9. T. Hauth, K. Pielmaier, V. Dieterich, N. Wein, H. Spliethoff, S. Fendt, Design parameter optimization of a membrane reactor for methanol synthesis using a sophisticated CFD model, Energy Advance, 4, 2025, 565-577.
10. T. Maier, M. Stripf, Distributed parameter model of a novel heat pump adsorber design using 3D-FEM, Applied Thermal Engineering, 278, 2025,